Electro-osmotic flow and the limiting current in alkaline water electrolysis

Haverkort, J. W.; Rajaei, H.

DOI
10.1016/j.powera.2020.100034

Publication date
2020

Document Version
Final published version

Published in
Journal of Power Sources Advances

Journal of Power Sources Advances 6 (2020) 100034

Contents lists available at ScienceDirect

Journal of Power Sources Advances

journal homepage: www.journals.elsevier.com/journal-of-power-sources-advances

Electro-osmotic flow and the limiting current in alkaline water electrolysis

J.W. Haverkort *, H. Rajaei

Process & Energy Department, Delft University of Technology, Leeghwaterstraat 39, 2628, CB Delft, the Netherlands

ARTICLE INFO

Keywords:
Alkaline water electrolysis
Limiting current density
Hydrogen purity
Microporous separator

ABSTRACT

Under alkaline conditions, hydroxide ions can deplete at the anode of a water electrolyser for hydrogen production, resulting in a limiting current density. We found experimentally that in a micro-porous separator, an electro-osmotic flow from anode to cathode lowers this limiting current density. Using the Nernst-Planck equation, a useful expression for the potential drop in the presence of diffusion, migration, and advection is derived. A quasi-stationary, one-dimensional model is used to successfully describe the transient dynamics. Electro-osmotic flow-driven cross-over of dissolved oxygen is argued to impact the hydrogen purity.

1. Introduction

The commercially most attractive way of producing green hydrogen is presently through the proven technology of alkaline water electrolysis [9,12,20,23,29]. Under alkaline conditions, water splitting proceeds through a reduction reaction $2H_2O + 2e^- \rightarrow 2OH^- + H_2$ and an oxidation reaction $2OH^- \rightarrow 2e^- + \frac{1}{2}O_2 + H_2O$. For this latter reaction to proceed in steady-state, hydroxide ions have to be transported from cathode to anode through a thin porous diaphragm or separator that avoids mixing of hydrogen and oxygen bubbles [9,20,23,29]. When reactants cannot be transported sufficiently fast, a maximum or *limiting current* exists [6,16,19,28]. Self-ionization of water cannot supply the required hydroxide at the anode because, in the typically used electrolyte KOH there is no other anion besides OH^- that can ensure charge-neutrality. In this work we experimentally demonstrate this theoretically expected limiting current for the first time. The impact of induced electro-osmotic flows [3] is investigated through useful analytical expressions for the potential drop that include advection.

2. Model equations

We consider a near-neutral diaphragm with pores large enough to neglect the surface-charge concentration compared to electrolyte concentration [1,5], so that surface conduction can be neglected [16,18]. The pores are however small enough to allow for an averaged description over many pores and avoid electro-osmotic instabilities [3,10,21,22] giving rise to overlimiting currents [6]. We assume an incompressible, dilute, quasi-neutral, binary, monovalent electrolyte with molar concentration c and electrostatic potential ϕ, moving with a constant superficial velocity u in the x-direction. The x-coordinate runs through the separator from $x = 0$ on the left to $x = L$ on the right, as shown in Fig. 1. The conserved molar fluxes of the cations (K^+) and anions (OH^-) in the x-direction, N_+ and N_- respectively (see Fig. 2), satisfy the 1D Nernst-Planck equation [17]:

$$N_\pm = uc - D_\pm\left(c' \pm c\frac{F\phi'}{RT}\right). \tag{1}$$

Here, a prime denotes a derivative with respect to x, D_+ and D_- are the effective porous medium ion diffusivities and $RT/F \approx 26$ mV at room temperature T, using the gas constant R, and Faraday constant F. The conserved current density $i \equiv F(N_+ - N_-)$ and molar "salt flux" N

$$N \equiv \frac{D_-N_+ + D_+N_-}{D_+ + D_-} = N_+ - \frac{D_+}{D_+ + D_-}\frac{i}{F}, \tag{2}$$

can, with some algebra, be written as

$$i = -\kappa(\phi + \chi(\ln c))', \tag{3}$$

$$N = uc + D_a c' = N_{\lim}\left(1 - \frac{c_l}{c_r}e^{\mathrm{Pe}}\right). \tag{4}$$

Here the ionic conductivity $\kappa \equiv \frac{F^2}{RT}(D_+ + D_-)c$, the ambipolar diffusivity $D_a \equiv \frac{2D_+D_-}{D_+ + D_-}$, and the parameter $\chi \equiv \frac{D_+ - D_-}{D_+ + D_-}\frac{RT}{F} \approx -12$ mV for KOH at room temperature.

The second equality in Eq. (4) was obtained by inserting the well-

* Corresponding author.
E-mail address: J.W.Haverkort@tudelft.nl (J.W. Haverkort).

https://doi.org/10.1016/j.powera.2020.100034
Received 12 June 2020; Received in revised form 25 September 2020; Accepted 26 September 2020

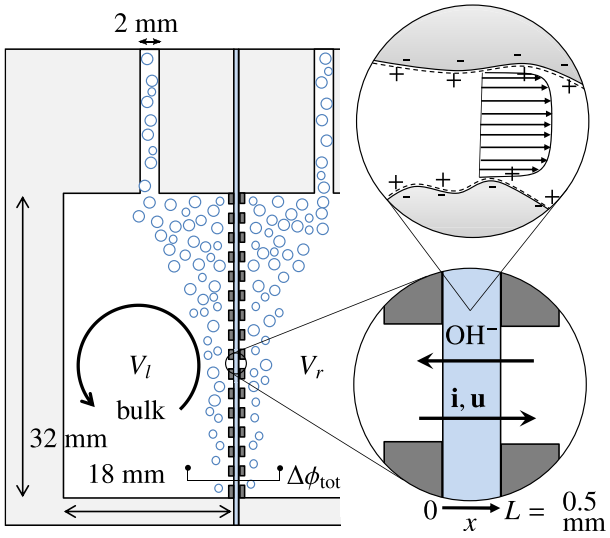

Fig. 1. A schematic depiction of the geometry, dimensions, and coordinate system used in the experiments and analysis. On the left, oxygen bubbles evolve from the expanded metal anode while at the cathode on the right of the separator, hydrogen is produced. The measured potential drop $\Delta\phi_{tot}$, left and right volume V_l and V_r, and the direction of the current density **i** and velocity **u** are indicated.

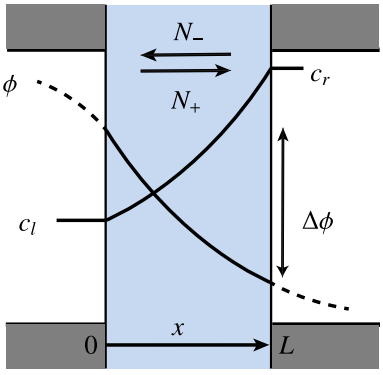

Fig. 2. Idealized average profiles of the electrolyte concentration c, potential ϕ, and the direction of fluxes of hydroxide anions, N_- , and potassium cations, N_+.

known solution to the advection-diffusion equation $N' = 0$:

$$c(x) = c_l + (c_r - c_l)\frac{e^{\mathrm{Pe}(x/L)} - 1}{e^{\mathrm{Pe}} - 1}, \tag{5}$$

that satisfies the boundary conditions $c(0) = c_l$ on the left and $c(L) = c_r$ and right, respectively. The Péclet number $\mathrm{Pe} \equiv uL/D_a$ is positive for a flow in the positive x-direction, from left to right. The concentration c_l tends to zero when N approaches the limiting flux $N_{\lim} \equiv -\frac{D_a c_r}{L}\frac{\mathrm{Pe}}{e^{\mathrm{Pe}}-1}$. Since K^+ is not involved in the reaction, when the advective flux vanishes in steady-state electrolysis, the diffusion flux cancels the migration flux to give $N_+ = 0$. This common case of an unsupported binary electrolyte is treated in many textbooks, see for example Ref. [14]. From Eq. (2), i thus becomes proportional to N, resulting in a limiting current density $i_{\lim} = \frac{2FD_- c_r}{L}\frac{\mathrm{Pe}}{e^{\mathrm{Pe}}-1}$, as was first derived in Ref. [28]. Here, the factor two is due to migration. The advective flux of a flow to the right opposes the diffusion flux to the left, *lowering* the limiting current by the factor $\frac{\mathrm{Pe}}{e^{\mathrm{Pe}}-1} < 1$.

Integrating Eq. (3), using Eq. (5), gives for $-\Delta\phi \equiv \phi(0) - \phi(L)$:

$$-\Delta\phi = \left(\chi - \frac{iL}{\kappa_c \mathrm{Pe}}\right)\ln\left(\frac{c_r}{c_l}\right) + \frac{iL}{\kappa_c}, \tag{6}$$

$$= \left(\chi - \frac{iL}{\kappa_c \mathrm{Pe}}\right)\ln\left(\frac{1}{1 - \frac{N}{N_{\lim}}}\right) + \chi\mathrm{Pe}, \tag{7}$$

where the characteristic quantity $\kappa_c \equiv \frac{N}{uc}\kappa = \frac{\kappa_l e^{\mathrm{Pe}} - \kappa_r}{e^{\mathrm{Pe}}-1}$ tends to the upstream conductivity when $|\mathrm{Pe}| \gg 1$. The ohmic contributions, proportional to i, are impacted by advection through the concentration profile. The diffusion potential, proportional to χ, will oppose the ohmic drop when $\chi(c_r - c_l)/i < 0$.

Surprisingly, Eqs. (6) and (7) for the potential drop in the presence of diffusion, migration, and advection do not seem to have been previously reported in this general form. See, however, Ref. [30] for when $i = 0$, relevant to filtration or reverse osmosis, or Refs. [19,28] for when $N_+ = 0$ or $N_- = 0$, relevant as an approximation near an ion-selective membrane. Expressions for charged media, sometimes including ion hindrance or reflection, also exist [11,13,24] but do not easily simplify to our case of negligible fixed charge. In Ref. [1] we generalize Eqs. (6) and (7) to apply to a binary electrolyte with arbitrary valencies.

When the flow is electro-osmotically driven, the superficial velocity $u = -\mathscr{M}\frac{\Delta\phi}{L}$ will be proportional to the average electric field $-\Delta\phi/L$ so that

$$\mathrm{Pe} = -\frac{\mathscr{M}}{D_a}\Delta\phi. \tag{8}$$

The effective electro-osmotic mobility $\mathscr{M}$ is related through the Helmholtz-Smoluchowski relation [3,6,8,16] $\mathscr{M} = -\epsilon\frac{\varepsilon_r\varepsilon_0\zeta}{\mu}$ to the zeta potential ζ. Here $\varepsilon_r\varepsilon_0$ is the electrical permittivity, μ is the liquid dynamic viscosity, and ϵ is the porosity; present since the Péclet number is based on the superficial velocity.

To solve Eq. (8) and Eq. (6) self-consistently, requires a model for c_l and c_r. We assume a perfectly mixed anolyte of volume V_l and catholyte of volume V_r, both much larger than the separator volume, see Fig. 1. For times t much larger than the diffusional time-scale the above equations will approximately hold quasi-stationary. The conservation equations of the non-reacting cation (K^+) and anolyte volume read, with A the separator area,

$$\frac{d(c_l V_l)}{dt} = -AN_+, \quad \frac{dV_l}{dt} = -uA. \tag{9}$$

With initial conditions $V_l = V_r = V_0$ and average concentration $c_0 = \frac{c_l V_l + c_r V_r}{2V_0}$, Eq. (4) and Eq. (2) combine to give, with some algebra,

$$\frac{dc_l}{dt} = \frac{c_0(1 - i/i_{\lim}) - c_l}{\tau}. \tag{10}$$

Here, the equilibration time τ and limiting current density $i_{\lim}$ are given by

$$\tau \equiv \frac{V_l V_r}{V_0^2}\frac{e^{\mathrm{Pe}} - 1}{\mathrm{Pe}}\tau_0, \quad \tau_0 \equiv \frac{LV_0}{2AD_a}, \tag{11}$$

$$i_{\lim} \equiv \frac{V_0}{V_r}\frac{\mathrm{Pe}}{e^{\mathrm{Pe}} - 1}i_0, \quad i_0 \equiv \frac{4FD_- c_0}{L}. \tag{12}$$

When $\mathrm{Pe} \ll 1$ we see, with $\frac{e^{\mathrm{Pe}}-1}{\mathrm{Pe}} \approx 1 + \mathrm{Pe}/2 + \mathscr{O}(\mathrm{Pe}^2)$, that initially $\tau \approx \tau_0$ is much smaller than the time V_0/uA it takes to drain the volume and, for negligible separator volume $AL \ll V_0$, much larger than the diffusive time-scale, given in Ref. [2] as $L^2/4D_a$. Note that under these conditions water electrolysis could be used to desalinate ($c_l \approx 0$) and

concentrate binary solutions like KOH or caustic soda, NaOH, without the use of ion-selective membranes or pumps. When $c_l = 0$ we have $2c_0V_0/V_r = c_r$ so that Eq. (12) agrees with the expression for $i_{\lim}$ discussed above.

A numerical solution to the coupled Eqs. 8–10 is shown in Fig. 3. As c_l decreases and c_l increases, $-\Delta\varphi$ initially very slightly decreases due to the diffusion potential in Eq. (6). As c_l and κ_c continue to decrease, $-\Delta\varphi$ starts to increase, increasing the electro-osmotic flow velocity. As $c_l \to 0$ the draining accelerates and as $V_l \to 0$ an associated rapid decrease in c_r can be seen.

3. Experimental results

The geometry of Fig. 1 was constructed from several laser-cut layers of plexiglass separated by Agfa's Zirfon (R) Perl UTP 500 [20,23,29]. This separator consists of 85 w% ZrO_2 particles on a 15 w% polysulfone backbone and has an average pore size of 0.15 ± 0.05 μm, a porosity of $\epsilon \approx 50 \pm 10\%$ and a thickness of $L \approx 0.5 \pm 0.05$ mm. Roughly equally thick electrodes of $A = 32 \times 32$ mm^2 ≈10 cm^2 were positioned directly adjacent to the separator in a zero-gap configuration, and connected to a power source. Expanded mesh electrodes by Permascand were used, with proprietary coating and a fractional open area of roughly 1/3-rd, consisting of approximately ellipse-shaped holes of roughly 3×1 mm.

Parallel to the 32×2 mm^2 gas outlets shown in Figs. 1, 6×8 mm^2 bubble-free channels were constructed to determine the liquid level. An equal initial volume $V_l = V_r = 24$ ml of 0.1 M aqueous potassium hydroxide solution was used on both sides.

We assume a tortuosity of $\tau = 1.62 \pm 0.2$, in the range of values measured [20], so that upon multiplying the molecular hydroxide and potassium diffusivities [17] with $\epsilon/\tau \approx 0.31$ we obtain the effective values $(D_-, D_+, D_a) \approx (1.6, 0.61, 0.88) \times 10^{-9}$ m^2/s.

Upon application of a current density $i = i_0 = \frac{4FD_{-}c_0V_0}{L} = 12.6$ mA/cm^2 we found a flow velocity of $u \approx 1$ μm/s from anode to cathode so that Pe ≈ 0.6. Note that this flow direction is opposite to that expected from the consumption and production of water and that due to electro-osmotic drag of hydroxide ions. Fig. 4 shows the measured ionic potential difference $-\Delta\varphi_{\text{tot}}$ between the left and right bulk electrolyte of Fig. 1.

Fig. 4 shows the measured ionic potential difference $-\Delta\varphi_{\text{tot}}$ between the bulk anolyte and catholyte. A comparison with the $-\Delta\varphi$ of Eq. (6) is shown, solved numerically with Eqs. (8)-(12), to which we added an ohmic drop corresponding to an effective electrode thickness of $l_e \approx 0.3$ mm. Without additional parameter fitting, the time over which the limiting current condition is reached, is predicted accurately apart from a "negative lag-time" of approximately 10 minutes. Besides significant uncertainty in various input parameters this discrepancy may be, at least partly, due to our assumption of a quasi-steady state [1].

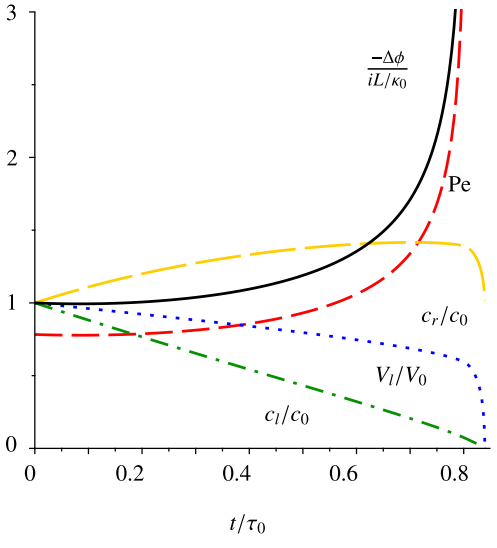

Fig. 3. Various dimensionless quantities as a function of dimensionless time t/τ_0, for $i/i_0 = 1.2$, obtained from the numerical solution of the coupled Eqs. (8) and (9) using the experimental values from Table 1. A slight initial decrease in $-\Delta\varphi$ can be seen, associated with the diffusion potential of Eq. (6). Later however, the decrease in κ_c makes that $-\Delta\varphi$ increases with time.

Table 1
Approximate experimental parameters values at $c_0 = 0.1$ M and $T = 298$ K. Other parameters include $RT/F \approx 26$ mV, $\chi \approx -12$ mV, transference number $t_+ = 1 - t_- = 0.27$, dynamic viscosity $\mu = 0.9$ mPas, relative permittivity $\varepsilon_r = 77$.

Porous medium correction ϵ/τ	$0.5/1.62 = 0.31$
Ambipolar diffusivity D_a	$0.88 \cdot 10^{-9}$ m^2/s
Separator thickness L	0.5 mm
Electrode/Separator area A	10 cm^2
Electro-osmotic mobility $\mathscr{M}$	$6.7 \cdot 10^{-9}$ m^2/s/V
At $t = 0$, for $i = i_0 = 12.6$ mA/cm^2	
Volume $V_l(0) = V_r(0) = V_0$	24 ml
Separator conductivity κ_0	0.84 S/m
Péclet number $\text{Pe}_0 = \frac{\mathscr{M} i_0 L}{\kappa_0 D_a}$	0.57
Limiting current density $i_{\lim}$	10 mA/cm^2
Time-scale $\tau = \frac{LV_0}{2AD_a} \frac{e^{\text{Pe}} - 1}{\text{Pe}}$	$8.9 \cdot 10^3$ s

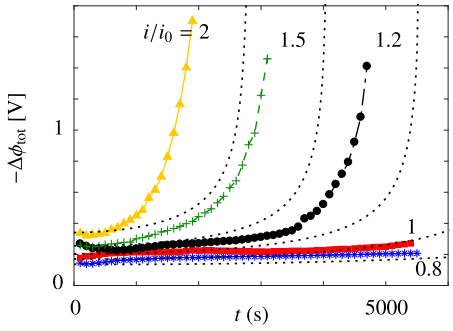

Fig. 4. The measured potential difference $-\Delta\varphi_{\text{tot}}$ between the left and right bulk electrolyte of Fig. 1, as a function of time t after switching on different values of the current density i/i_0. The dotted black lines represent $-\Delta\phi + il_e/\kappa_l + il_e/\kappa_r$ where $\Delta\varphi$, κ_l, and κ_r are obtained using the model equations and parameter values detailed in the caption of Fig. 3 using no fitting of parameters other than $l_e = 0.3$ mm. Reasonable agreement in the predicted limiting current can be seen.

We performed the same experiment for electrolyte concentrations of 0.1, 1, 2.9, and 5.7 M. We note that beyond approximately 1 M the conductivity no longer increases linearly with increasing concentration [7], resulting in the present dilute solution theory giving larger errors [1].

The effective zeta-potential shown in Fig. 5 was obtained from Eq. (8) with $-\Delta\phi/L = i/\kappa_0$ using for the conductivity the correlation from Ref. [7] corrected by $\epsilon/\tau \approx 0.31$. The superficial velocity u through the separator was directly obtained from the initial time-rate of change of the electrolyte levels.

Here, we did correct for the water consumed and produced in the reaction but not for any hydrostatic pressure-driven contribution induced by the change in levels over time. At elevated concentrations, electro-osmotic *drag* also causes a significant net water flux in the direction of the flux of hydroxide ions [1]. Note that despite all these opposing effects: water consumption, production, drag, *and* back-pressure, the net flow remained dominated by electro-osmosis and was always directed from anode to cathode.

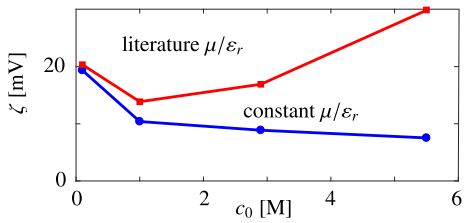

Fig. 5. The 'zeta potential' ζ calculated from Eq. (8) as $\zeta = -\mathscr{M}\mu/\epsilon\varepsilon_r\varepsilon_0$ where the electrical mobility $\mathscr{M} = u\kappa/i$ was determined from the experiments at $t =$ 150 s. Note that defined in this way, ζ is a rather effective empirical value, including the effect of electro-osmotic drag [1], and may differ substantially from the zeta-potential determined by different means. For the bottom curve, a constant viscosity to relative permittivity ratio $\mu/\varepsilon_r \approx 12$ μPas for water was used while for the top curve we used the experimental data from Refs. [15,27] as well as a quite uncertain quadratically extrapolated value of $\varepsilon_r = 40$ for the highest molarity.

4. Discussion

The observed electrolyte flow through the separator may transport dissolved reaction products, potentially adversely impacting safety, Faradaic efficiency, and gas purity. Therefore we would like to estimate these effects for a typical operating temperature of 80 °C. Using that in the range 1 M$\leq c_0 \leq$ 5.7 M of Fig. 5 an approximately constant electrical mobility $\mathscr{M} \approx 3 \cdot 10^{-9}$ m^2/s/V is found, we can write Eq. (8) as

$$\mathrm{Pe} \approx k\frac{\Delta\phi}{T}, \tag{13}$$

where $k \approx -10^3$ K/V and we used the constancy of $D\mu/T$, with μ the dynamic viscosity, implied by the Stokes-Einstein relation [8,23,25]. From Eq. (13), we find that Pe = 1 is obtained at a very high separator voltage around 0.35 V. The oxygen and hydrogen diffusivity in 30 w% KOH are approximately 2 and 6 times 10^{-9} m^2/s [4], respectively, well below the roughly $9 \cdot 10^{-9}$ m^2/s of KOH [12]. Therefore at $-\Delta\phi = 0.15$ V, associated with the high end of present-day operational current densities, the Péclet numbers for oxygen and hydrogen are approximately 1.8 and 0.6, respectively. We may use these values for Pe in Eq. (5) to describe gas cross-over. The diffusive transport of hydrogen to the anode, on the left of Fig. 1 where $c_l = 0$, will be reduced by the factor $\frac{\mathrm{Pe}}{e^{\mathrm{Pe}}-1} \approx 0.7$ appearing in Eq. (4). Similarly, the oxygen flux, with $c_r = 0$, will be $\frac{\mathrm{Pe}}{e^{\mathrm{Pe}}-1}e^{\mathrm{Pe}} \approx 2.2$ times higher compared to the case of only diffusion. At equal concentration of dissolved gases, electro-osmotic flows will then make cross-over of oxygen transport as significant as that of hydrogen, despite its three times smaller diffusivity. Since the solubility of oxygen exceeds that of hydrogen [26] these tentative conclusions warrant further investigation. Most studies so-far have however only considered hydrogen cross-over [9,23,29]. A relatively low oxygen in hydrogen content was measured in Ref. [9], although to an unknown degree this may be due to oxygen reacting back to water with hydrogen at the cathode. At the high current densities required for significant electro-osmotic flows, the concentration of oxygen in hydrogen will likely remain well below the lower explosion limit of around 4 v% [9]. Enhanced oxygen cross-over will however nonetheless impact the Faradaic efficiency [9,25] or hydrogen purity.

Finally, knowledge of these electro-osmotic flows may be actively used to influence the cross-over, allowing the development of thinner separators with reduced gas-cross over of at least one of the dissolved species, oxygen or hydrogen. The surface properties of separators may be modified to control the zeta potential. For some materials, a charge inversion can effectively change the direction of electro-osmotic flows [8]. Alternatively, a (hydrostatic) pressure difference can be applied to counteract electro-osmotic flow.

Declaration of competing interest

The authors declare that they have no known competing financial interests or personal relationships that could have appeared to influence the work reported in this paper.

Acknowledgements

We thank T.P.M. Hooijschuur, T.M. van Velzen and M.M. het Lam for their help with the experiments and Remco Hartkamp and Niels Boon for insightful discussions. We acknowledge funding support from Shell Global Solutions International B.V., The Netherlands, under agreement number PT73368.

References

[1] J.W. Haverkort, Modelling and experiments of binary electrolytes in the presence of diffusion, migration, and electro-osmotic flow, Phys. Rev. Appl. 14 (2020), 044047.
[2] V. M. Aguilella, S. Mafé, and J. Pellicer. Ionic transport through a homogeneous membrane in the presence of simultaneous diffusion, conduction and convection. J. Chem. Soc., Faraday Trans. 1 85(2):223–235.
[3] E. Boyko, R. Eshel, A.D. Gat, M. Bercovici, Nonuniform electro-osmotic flow drives fluid-structure instability, Phys. Rev. Lett. 124 (2) (2020), 024501.
[4] R. Davis, G. Horvath, C. Tobias, The solubility and diffusion coefficient of oxygen in potassium hydroxide solutions, Electrochim. Acta 12 (3) (1967) 287–297.
[5] E.V. Dydek, M.Z. Bazant, Nonlinear dynamics of ion concentration polarization in porous media: the leaky membrane model, AIChE J. 59 (9) (2013) 3539–3555.
[6] E.V. Dydek, B. Zaltzman, I. Rubinstein, D.S. Deng, A. Mani, M.Z. Bazant, Overlimiting current in a microchannel, Phys. Rev. Lett. 107 (11) (2011) 118301.
[7] R. Gilliam, J. Graydon, D. Kirk, S. Thorpe, A review of specific conductivities of potassium hydroxide solutions for various concentrations and temperatures, Int. J. Hydrogen Energy 32 (3) (2007) 359–364.
[8] R. Hartkamp, B. Siboulet, J.-F. Dufrêche, B. Coasne, Ion-specific adsorption and electroosmosis in charged amorphous porous silica, Phys. Chem. Chem. Phys. 17 (38) (2015) 24683–24695.
[9] P. Haug, M. Koj, T. Turek, Influence of process conditions on gas purity in alkaline water electrolysis, Int. J. Hydrogen Energy 42 (15) (2017) 9406–9418.
[10] A.S. Khair, Concentration polarization and second-kind electrokinetic instability at an ion-selective surface admitting normal flow, Phys. Fluids 23 (7) (2011), 072003.
[11] A.-K. Kontturi, K. Kontturi, J.A. Manzanares, S. Mafé, Equilibrium and transport properties of polydisperse polyelectrolytes in graft-modified porous charged membranes: forced permeation–diffusion of lignosulfonate, Phys. Chem. Chem. Phys. 1 (8) (1999) 1939–1945.
[12] D. Le Bideau, P. Mandin, M. Benbouzid, M. Kim, M. Sellier, Review of necessary thermophysical properties and their sensitivities with temperature and electrolyte mass fractions for alkaline water electrolysis multiphysics modelling, Int. J. Hydrogen Energy 44 (10) (2019) 4553–4569.
[13] X. Lefebvre, J. Palmeri, P. David, Nanofiltration theory: an analytic approach for single salts, J. Phys. Chem. B 108 (43) (2004) 16811–16824.
[14] C. Lefrou, P. Fabry, J.-C. Poignet, Electrochemistry: the Basics, with Examples, Springer Science & Business Media, 2012.
[15] A. Lileev, D. Loginova, A. Lyashchenko, Microwave dielectric properties of potassium hydroxide aqueous solutions, Russ. J. Inorg. Chem. 56 (6) (2011) 961–967.
[16] S. Nam, I. Cho, J. Heo, G. Lim, M.Z. Bazant, D.J. Moon, G.Y. Sung, S.J. Kim, Experimental verification of overlimiting current by surface conduction and electro-osmotic flow in microchannels, Phys. Rev. Lett. 114 (11) (2015) 114501.
[17] J. Newman, K.E. Thomas-Alyea, Electrochemical Systems, John Wiley & Sons, 2012.
[18] C.P. Nielsen, H. Bruus, Concentration polarization, surface currents, and bulk advection in a microchannel, Phys. Rev. 90 (4) (2014), 043020.
[19] V. Nikonenko, K. Lebedev, S. Suleimanov, Influence of the convective term in the nernst-planck equation on properties of ion transport through a layer of solution or membrane, Russ. J. Electrochem. 45 (2) (2009) 160–169.
[20] J. Rodríguez, S. Palmas, M. Sánchez-Molina, E. Amores, L. Mais, R. Campana, Simple and precise approach for determination of ohmic contribution of diaphragms in alkaline water electrolysis, Membranes 9 (10) (2019) 129.
[21] I. Rubinstein, B. Zaltzman, Equilibrium electroconvective instability, Phys. Rev. Lett. 114 (11) (2015) 114502.
[22] S.M. Rubinstein, G. Manukyan, A. Staicu, I. Rubinstein, B. Zaltzman, R.G.H. Lammertink, F. Mugele, M. Wessling, Direct observation of a nonequilibrium electro-osmotic instability, Phys. Rev. Lett. 101 (23) (2008) 236101.
[23] M. Schalenbach, W. Lueke, D. Stolten, Hydrogen diffusivity and electrolyte permeability of the Zirfon PERL separator for alkaline water electrolysis, J. Electrochem. Soc. 163 (14) (2016) F1480–F1488.
[24] R. Schlögl, Membrane permeation in systems far from equilibrium, Ber. Bunsen Ges. Phys. Chem. 70 (4) (1966) 400–414.
[25] T. Shinagawa, K. Takanabe, Towards versatile and sustainable hydrogen production through electrocatalytic water splitting: electrolyte engineering, ChemSusChem 10 (7) (2017) 1318–1336.

[26] S. Shoor, R.D. Walker Jr., K. Gubbins, Salting out of nonpolar gases in aqueous potassium hydroxide solutions, J. Phys. Chem. 73 (2) (1969) 312–317.
[27] P.M. Sipos, G. Hefter, P.M. May, Viscosities and densities of highly concentrated aqueous MOH solutions (M+= Na+, K+, Li+, Cs+,(CH3) 4N+) at 25.0 ° C, J. Chem. Eng. Data 45 (4) (2000) 613–617.
[28] Y. Tanaka, Concentration polarization in ion exchange membrane electrodialysis, J. Membr. Sci. 57 (2–3) (1991) 217–235.
[29] P. Trinke, P. Haug, J. Brauns, B. Bensmann, R. Hanke-Rauschenbach, T. Turek, Hydrogen crossover in PEM and alkaline water electrolysis: mechanisms, direct comparison and mitigation strategies, J. Electrochem. Soc. 165 (7) (2018) F502–F513.
[30] M. Vonk, J. Smit, The application of generalized Nernst-Planck equations to the description of ion retention in the hyperfiltration of mixed electrolyte solutions through a neutral membrane, Ber. Bunsen Ges. Phys. Chem. 88 (8) (1984) 724–732.